Cellular/Molecular

An Acute Effect of Neuregulin 1β to Suppress α7-Containing Nicotinic Acetylcholine Receptors in Hippocampal Interneurons

Qing Chang and Gerald D. Fischbach
Department of Pharmacology, College of Physicians and Surgeons, Columbia University, New York, New York 10032

We examined rapid effects of neuregulin (NRG) on nicotinic acetylcholine (ACh) receptors in interneurons located in the stratum radiatum of the hippocampus. Two types of response were detected by whole-cell recordings after brief pulses of ACh. One type was a rapidly rising and falling (monophasic) current that was blocked by methyllycaconitine. The other type was a similar fast response followed by a more slowly rising and falling current. The slow component of the biphasic response was resistant to methyllycaconitine. Perfusion or local application with NRG 1β rapidly decreased fast inward ACh currents. NRG 1β had no effect on slow responses. NRG 1β suppression was abolished by the ErbB tyrosine kinase inhibitor PD 158780 (4-[(3-bromophenyl) amino]-6-(methylamino)-pyrido[3,4-d]pyridimine). The NRG 1β effect was also inhibited by phalloidin and cytochalasin D. Furthermore, NRG 1β decreased the number of surface Alexa Fluor 488 α-bungarotoxin binding sites. We believe that the NRG 1β-induced inhibition of ACh currents is because of receptor internalization trigged by protein tyrosine phosphorylation. Significantly, fast nicotinic EPSCs evoked in the presence of muscarinic, ionotropic glutamate, and GABA receptors antagonists were also reduced by NRG 1β. Thus, short-term as well as long-term effects of NRG must be taken into consideration in studies of ACh receptor-mediated synaptic efficacy in the CNS.

Key words: **neuregulin; ErbB receptor; nicotinic acetylcholine receptor; hippocampus; interneurons; synaptic transmission**

Introduction

Neuregulins (NRGs) are a family of proteins encoded by four genes, *NRG 1–NRG 4*, that activate receptor tyrosine kinases that are related to the epidermal growth factor (EGF) receptor. The structure and function of proteins encoded by the *NRG 1* gene have been characterized most extensively (for review, see Buonanno and Fischbach, 2001; Falls, 2003; Talmage and Role, 2004).

ARIA (acetylcholine receptor inducing activity), a product of the *NRG 1* gene, was purified from chick brain based on its ability to increase the synthesis of muscle acetylcholine receptors (AChRs) (Usdin and Fischbach, 1986; Falls et al., 1993). NRG 1 proteins were subsequently found to increase the amplitudes of nicotinic ACh currents in neurons dissociated from the rat interpeduncular nucleus (Wietasch, 1997), chick sympathetic ganglia (Yang et al., 1998), and interneurons dissociated from the rat hippocampus (Liu et al., 2001). In the interpeduncular and hippocampal neurons, pharmacological data indicated that nicotinic AChRs (nAChRs) containing the α7 subunits were affected selectively.

The increase in receptor number and ACh currents in muscle and neurons were long-term effects in that they were measured after 1 d or more exposure to NRG 1. In this paper, we investigated more rapid "acute" effects of NRG 1 on α7 ACh currents in hippocampal interneurons. These GABAergic interneurons are extremely sensitive to ACh and they exhibit a relatively high density of α7 containing nAChRs (Jones and Yakel, 1997; Frazier et al., 1998a; Sudweeks and Yakel, 2000). NRG 1 is expressed in the hippocampus (Corfas et al., 1995; Law et al., 2004; Okada and Corfas, 2004) and in the medial septal nucleus (Corfas et al., 1995) whose axons project to the hippocampus. ErbB4 receptors are highly expressed in hippocampal interneurons (Garcia et al., 2000; Huang et al., 2000; Gerecke et al., 2001; Okada and Corfas, 2004).

The acute effect of NRG 1 on hippocampal interneurons, like the long-term effect, was selective for α7 nAChRs. In contrast to the long-term effect, the rapid action of NRG 1 resulted in a decrease rather than an increase in the α7 responses. In addition, we found that NRG 1 suppressed EPSCs that were mediated by α7 nAChRs.

Materials and Methods

Slice preparation and electrophysiology. All procedures involving animals were performed in accordance with Columbia University guidelines. Young (14- to 21-d-old) male CD1 mice were decapitated, and their brains were rapidly removed and placed into ice-cold dissecting solution [in mM: 40 NaCl, 25 $NaHCO_3$, 10 D-glucose, 150 sucrose, 4 KCl, 1.25 NaH_2PO_4, 0.5 $CaCl_2$, and 7 $MgCl_2$ (saturated with 95% O_2/5% CO_2)]. Horizontal brain slices (350 μm thick) containing the hippocampus were cut on a vibratome (VT 1000S; Leica, Nussloch, Germany) and transferred into a holding chamber containing artificial CSF (ACSF) [in mM: 124 NaCl, 25 $NaHCO_3$, 25 D-glucose, 3 KCl, 1.25 NaH_2PO_4, 2 $CaCl_2$, and 1 $MgCl_2$ (bubbled with 95% O_2/5% CO_2)]. For the recording of nAChR-

Received April 27, 2006; revised Sept. 15, 2006; accepted Sept. 15, 2006.
We thank Dr. Mary Ann Mann and Jinghua Zhang for technical assistance.
Correspondence should be addressed to Dr. Gerald D. Fischbach, Department of Pharmacology, Columbia University, 630 West 168th Street, New York, NY 10032. E-mail: gdf@columbia.edu.
DOI:10.1523/JNEUROSCI.1794-06.2006
 0270-6474/06/2611295-09$15.00/0

mediated EPSCs, young (16- to 27-d-old) male Sprague Dawley rats were used to cut 350-μm-thick coronal slices. After a 1 h recovery at 35°C, slices were allowed to cool down to room temperature (22–24°C), transferred to a chamber mounted on the fixed stage of an upright microscope, and superfused continuously with room temperature ACSF at a rate of 2 ml/min. In all of the experiments, 1–5 μM atropine sulfate was added to the bath solution to block muscarinic AChRs. Hippocampal interneurons were visualized on a video monitor through an infrared-differential interference contrast (IR-DIC)-sensitive camera (MacVicar, 1984; Dodt and Zieglgansberger, 1990). Whole-cell patch-clamp recordings were made with glass pipettes pulled on a Flaming/Brown electrode puller (Sutter Instruments, Novato, CA). The resistance of the pipettes was 2–6 MΩ when filled with an intracellular solution (in mM: 135 Cs-methanesulphonate, 10 HEPES, 1 EGTA, 7 NaCl, 2 MgATP, 0.3 NaGTP, and 5 QX-314 [*N*-(2, 6-dimethylphenylcarbamoylmethyl) triethylammonium bromide], pH 7.3). In some experiments, 0.1% biocytin was included in the pipette solution for subsequent visualization of the cell morphology. Currents from interneurons were monitored with an Axopatch 200A amplifier (Molecular Devices, Palo Alto, CA), acquired through Digidata 1322A (Molecular Devices) onto a Pentium computer using pClamp 9 software (Molecular Devices). Peak amplitudes were measured using Mini Analysis software (Synaptosft, Decatur, GA). Data are reported as mean ± SEM.

ACh was applied through a small tipped (<1 μm) pipette that was moved under visual control to within ~30 μm of the soma of the neuron under study. The ACh solution was pressure ejected (10 ms, 10 psi) directly onto the cell body and proximal dendrites using a Picospritzer (General Valve, Fairfield, NJ). The pipette solution contained 1 mM ACh dissolved in ACSF, pH 7.4, as described above, except that HEPES was substituted for $NaHCO_3$.

For the recording of nAChR-mediated EPSCs, 6-cyano-7-nitroquinoxaline-2–3-dionedisodium (CNQX) (20 μM), 2-amino-5-phosphonopentanoic acid (APV) (50 μM), and picrotoxin (100 μM) were added to bath solution to block glutamatergic and GABAergic activity. Evoked synaptic currents were induced in response to a 30 V, 50 μs stimulus applied at 0.016 Hz via a concentric bipolar stimulating electrode (Frederick Haer Company, Bowdoinham, ME) that was positioned under visual guidance in either stratum radiatum (SR) or stratum oriens (SO).

Cell culture and whole-cell patch-clamp recording. Hippocampal neuron cultures were prepared from the newborn CD1 mice. Hippocampi were dissected out, minced, and incubated with 0.25% trypsin (Invitrogen, Carlsbad, CA) for 20 min at 37°C. Using a sterile Pasteur pipette, neurons were dispersed and then plated on poly-L-lysine/laminin-coated coverslips. On the second day after plating, uridine and 5-fluoro-2-deoxyuridine were added to the culture medium to inhibit the proliferation of non-neuronal cells. For this study, the neurons were cultured for 14–30 d.

Whole-cell patch-clamp recording was performed on large neurons (≥20 μm across) (Liu et al., 2001) using the standard voltage-clamp technique. The signals were filtered at 2 kHz using an Axopatch 200B amplifier (Molecular Devices). Cells were superfused at a rate of 2 ml/min with an external bath solution containing the following (in mM): 150 NaCl, 2.5 KCl, 10 HEPES, 10 D-glucose, 2 $CaCl_2$, and 1 $MgCl_2$, pH 7.3–7.4. In cell cultures, NRG (5 nM) was applied locally by pressure ejection (100 ms, 10 psi) from one barrel of an electrode constructed from theta glass tubing (Warner Instruments, Hamden, CT). ACh (10 ms, 10 psi) was applied from the other barrel. The tip diameter of the theta glass pipette was ~10 μm and was placed 30–40 μm of the neuron under study.

Histology. Standard histological processing was performed to visualize the interneurons filled with biocytin. Briefly, slices were fixed overnight in a 0.1 M PBS containing 4% paraformaldehyde. Sections were permeabilized with 0.4% Triton X-100, treated with 0.3% hydrogen peroxide to reduce background peroxidase activity, and incubated overnight in avidin–biotin–peroxidase complex (Vector Laboratories, Burlingame, CA). The next day, the sections were stained with diaminobenzidine (Vector Laboratories) and mounted on slides.

Photomicrographs of biocytin-labeled cells and dendrites were taken using a Nikon (Melville, NY) E800 microscope equipped with a *z*-axis stage and a 20× DIC lens.

Labeling surface α7 nAChRs. Alexa Fluor 488 α-bungarotoxin (Alexa488-αBgt) (Invitrogen) was used to label surface α7 nAChRs on live hippocampal neurons. Cells maintained for 14–30 d in culture were treated for 9 min with or without 5 nM NRG 1β in the absence or presence of PD 158780 (4-[(3-bromophenyl) amino]-6-(methylamino)-pyrido[3,4-*d*]pyridimine) (10 μM) in Neurobasal medium plus 0.1% BSA and then incubated in the same medium containing 100 nM Alexa488-αBgt at 37°C for 45 min. Nonspecific binding was assessed by incubating the cells in αBgt (5 μM) 10 min before and during the labeling with Alexa488-αBgt. The cells were then washed four times in 2 ml of Neurobasal medium and fixed for 20 min at room temperature in 4% paraformaldehyde in PBS.

Fluorescence immunocytochemistry. For immunolabeling, fixed cells were permeabilized with 0.1% Triton X-100 in PBS and then incubated with a goat anti-α7-nAChR polyclonal antibody (SC1447, 1:1000 dilution in 0.1% Triton X-100 PBS; Santa Cruz Biotechnology, Santa Cruz, CA) at 4°C overnight. Nonspecific antibody binding was minimized by treatment with 5% donkey serum in PBS for 30 min at room temperature. Negative controls were assessed by first incubating the primary antibody with a fivefold excess of blocking peptide (SC1447P; Santa Cruz Biotechnology) for 2 h at room temperature and then incubating the mixture with the cells at 4°C overnight. Cells were washed three times in PBS and then incubated for 1 h at room temperature with a secondary antibody, rhodamine red-X-conjugated donkey anti-goat IgG (1:200 dilution in 0.1% Triton X-100 PBS; Jackson ImmunoResearch, West Grove, PA). The cells were then washed three times in PBS and mounted using anti-fade mounting solution (Vectashield; Vector Laboratories).

Image acquisition and quantification. Labeled cells were imaged using a 100× oil immerged objective (1.3 numerical aperture lens) mounted on

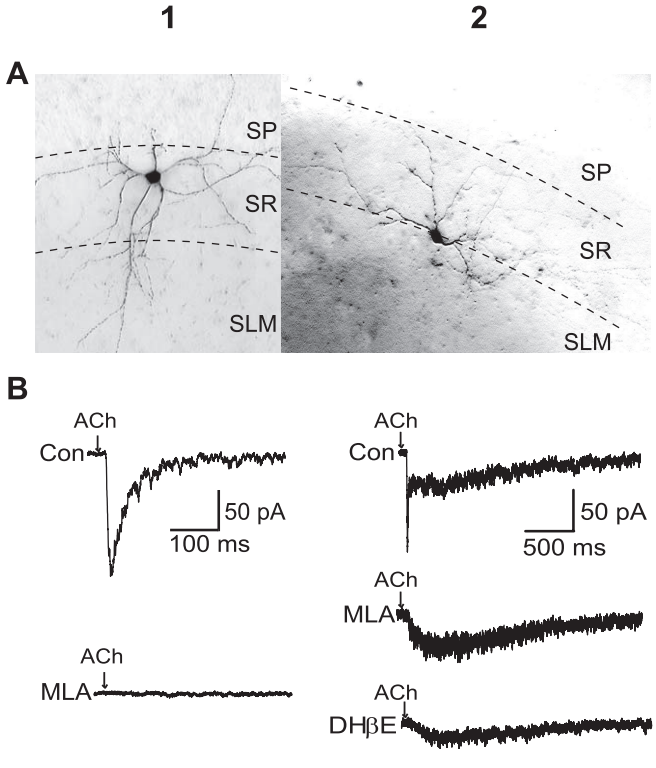

Figure 1. ACh currents evoked in mouse hippocampal CA1 interneurons. ***A***, Images of biocytin-injected interneurons in the middle of the SR (***A1***) and near the SR/SLM border (***A2***). ***B1***, In mid-SR interneurons, a 10 ms pulse of ACh produced a rapidly rising and decaying inward current (top trace) that was blocked by 10 nM MLA (bottom trace). ***B2***, At the SR/SLM border, most interneurons exhibited a fast current followed by a slower response (top trace). The fast component but not the slower response was blocked by MLA (middle trace). The slower component was reduced by DHβE (bottom trace). Con, Control.

Table 1. Distribution of nAChR actions in CA1 stratum radiatum of the hippocampus

	Middle of SR		Border of SR/SLM	
Response	Number of neurons	Peak amplitude of I_{Ach} (pA) (mean ± SEM)	Number of neurons	Peak amplitude of I_{Ach} (pA) (mean ± SEM)
Fast only	40	138.1 ± 11.3	12	125.3 ± 13.5
Fast and slow	8	95.1 ± 14.2 and 35.2 ± 4.3	32	93.6 ± 13.4 and 32.4 ± 4.6
None	3		1	
Total	51		45	

Pressure ejection was used to apply 1 mM ACh (10 ms, 10 psi) to CA1 interneurons. Atropine (1 μM) was included in the bath solution to block muscarinic responses. Holding potential, −65 mV.

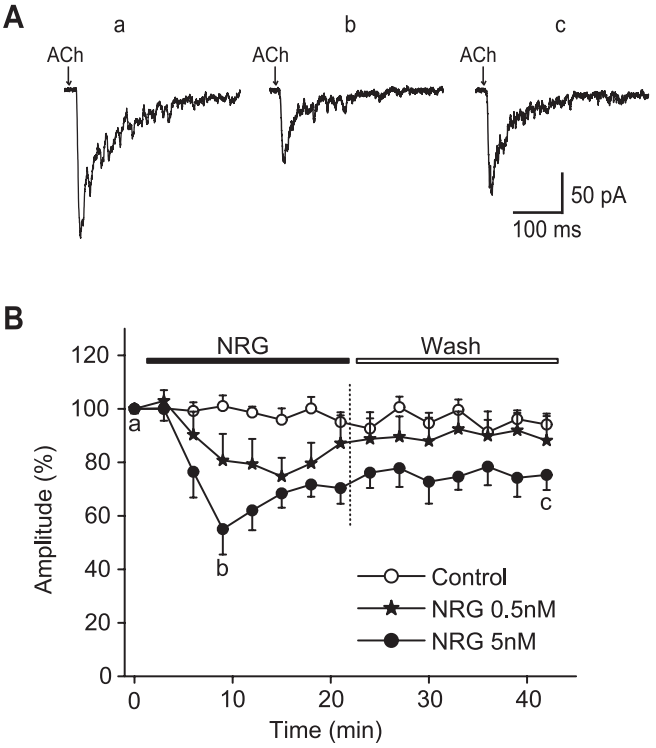

Figure 2. NRG 1β suppressed ACh-induced fast α7 currents. ***A***, Sample recordings of ACh-evoked fast currents before (***a***), 9 min after bath perfusion with 5 nM NRG 1β (***b***), and 21 min after washout of NRG 1β (***c***). ***B***, Fast inward current amplitudes (percentage) plotted versus time (minutes) in controls and in the presence of two different concentrations of NRG 1β (0.5 and 5 nM). The peak amplitude of each response was normalized to the initial response ($T = 0$) from the same cell in each case. Each point and bar represent mean and SEM, respectively, of results obtained from six neurons. Note that the peak amplitudes of ACh currents began to recover during the application of NRG 1β.

a Zeiss LSM 510 confocal microscope. All specimens were imaged under identical conditions and analyzed using identical parameters. Four to six independent experiments for each of the treatments were performed. On each coverslip, four to six neurons were quantified. Levels of surface and total α7 nAChRs fluorescence intensity on the same length of dendrites and the same area of somas in cells treated with various agents were compared using NIH Image J software. The surface-to-total ratio was determined by dividing the computed green fluorescence (surface receptors) by the red fluorescence (total receptors).

Measurements of surface cluster numbers were performed using NIH Image J software. For each neuron, the clusters of soma (within two 15 × 15 μm areas) and two to four dendrites (within 50 μm starting from the soma) were measured. Threshold values of 0.05 μm^2 and 50% of maximal intensity were chosen for defining clusters.

Results are presented as mean ± SEM. Statistical significance was determined by Student's *t* test.

Reagents. Recombinant human NRG 1β1/heregulin 1β1 EGF domain (amino acid residues 176–246) was purchased from R & D Systems (Minneapolis, MN). This NRG peptide is essential for all known biological activities and is necessary and sufficient for ErbB receptor activation (Lemke, 1996; Fischbach and Rosen, 1997). We will refer to it simply as "NRG 1β". PD 158780 was purchased from EMD Biosciences (San Diego, CA). QX-314-Cl was purchased from Alomone Labs (Jerusalem, Israel). All other chemicals were purchased from Sigma (St. Louis, MO). All drugs and solutions were made fresh from drug stock solutions and dissolved in an external bath solution.

Results

Two types of ACh response in CA1 stratum radiatum interneurons

There are many types of interneurons in the SR (Freund and Buzsaki, 1996). A previous study in rat hippocampal slices showed cell bodies and dendrites of interneurons near the SR/stratum lacunosum moleculare (SLM) border were oriented in a horizontal direction, whereas cells located in the middle of the SR between the SLM and the stratum pyramidale (SP) were more polygonal in shape and vertically oriented (Pawelzik et al., 2002). We observed the same tendency in mice after injecting SR interneurons with biocytin (Fig. 1*A*). Differences in cell body orientation were also evident under IR-DIC illumination, although exceptions were noted at each location (data not shown).

Pressure ejection was used to apply 10 ms pulses (10 psi) of 1 mM ACh to CA1 SR interneurons. A whole-cell patch-clamp recording from a neuron located in the mid-SR is shown in Figure 1*B1*. When the membrane potential was held at −65 mV, the ACh pulse produced a rapidly rising and rapidly decaying inward current (Fig. 1*B1*, top trace). Most interneurons located at the SR/SLM border responded to the 10 ms ACh pulse with a more complex response (Fig. 1*B2*). A fast inward current was followed by a slower response that peaked ~100 ms later and lasted longer than 1 s (Fig. 1*B2*, top trace). Results from 96 neurons are summarized in Table 1. Cell body position within the SR did not affect the magnitude of fast or slow responses. Rather, positional effects are evident in the relative frequencies of the responses.

Inward currents after ACh application were not affected by the voltage-dependent sodium channel blocker tetrodotoxin (500 nM). Also, ACh-induced currents were not affected by the ionotropic glutamate receptor antagonist CNQX (20 μM) and APV (50 μM) or the $GABA_A$ receptor antagonist picrotoxin (100 μM; data not shown). Therefore, the ACh responses are likely attributable to direct activation of postsynaptic nAChRs. This is consistent with previous reports (Frazier et al., 1998a; McQuiston and Madison, 1999).

Fast monophasic currents and the fast components of the biphasic responses were completely blocked by 10 nM methyllycaconitine (MLA), a selective α7 nAChR antagonist (Fig. 1*B1*,*B2*). The slower component was unaffected by MLA but was partially blocked by 100 nM dihydro-β-erythroidine (DHβE), a less selective nicotinic antagonist (Fig. 1*B2*). The slow component is probably attributable to activation of non-α7-containing nAChRs. Current–voltage relationships for both fast and slow ACh-evoked responses demonstrated strong inward rectification at positive

membrane potentials (supplemental Fig. S1, available at www.jneurosci.org as supplemental material) (Frazier et al., 1998a; McQuiston and Madison, 1999).

ACh-induced currents recorded in this study were small compared with the currents previously recorded in our laboratory using a U-tube method for rapid ACh application (Liu et al., 2001). The difference is likely attributable to the lower concentration of applied ACh (1 mM), the small tip of the ejection pipette, and the brevity of the pulses (10 ms) used in current experiments.

NRG 1β inhibited fast α7 responses

Perfusion of hippocampal slices with NRG 1β at 5 nM decreased ACh-evoked α7 responses in interneurons showing simple fast responses (Fig. 2) and in neurons that showed biphasic responses (Fig. 3). At 5 nM NRG 1β, inhibition was evident within 6 min of the onset of bath perfusion. Maximal inhibition in neurons that exhibited monophasic responses approached 45% (Fig. 2). The amplitude of the fast responses began to recover during the next 12 min, even in the continued presence of NRG 1β. After ~20 min of washout of NRG 1β, complete recovery of ACh responses from NRG 1β exposure was not achieved. Bath application of 0.5 nM NRG 1β produced a smaller but a significant inhibition (Fig. 2*B*). The onset of the inhibitory effect appeared to occur at a later time, and the maximal NRG 1β effect was achieved more slowly than at the higher dose (5 nM). Responses did return to control values after application of the lower dose.

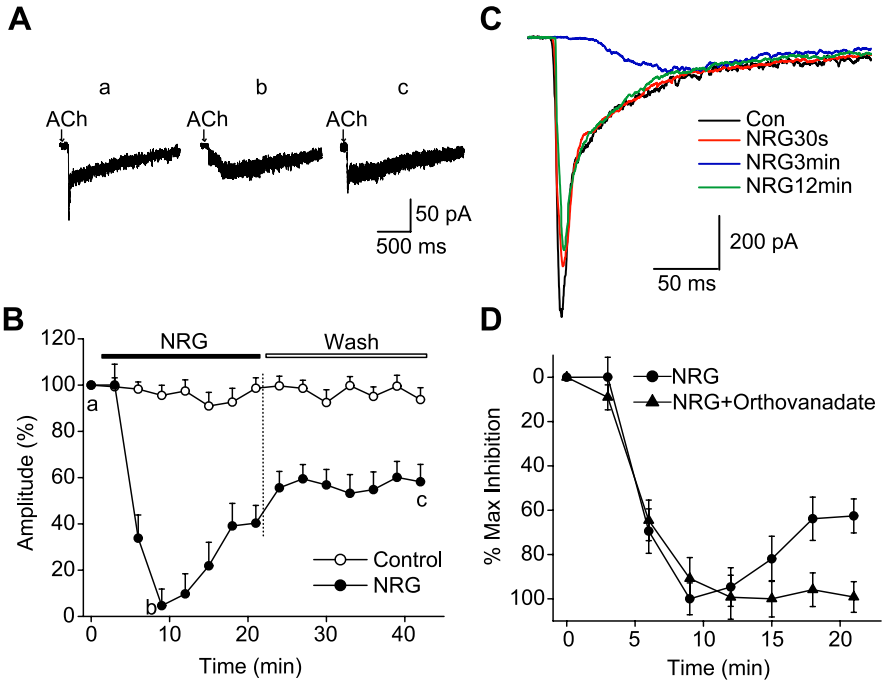

Figure 3. Effects of NRG 1β (5 nM) on biphasic nicotinic ACh currents. ***A***, Representative traces taken before (***a***), 9 min after NRG 1β perfusion (***b***), and 21 min after washout (***c***). ***B***, Averaged fast (α7) component amplitudes (percentage of $T = 0$; mean ± SEM; $n = 6$ cells) plotted versus time (minutes) in controls and in the presence of NRG 1β. In these cells, suppression of the fast currents was nearly complete. ***C***, Time course of NRG 1β effect on ACh-induced fast responses in hippocampal cell cultures. Sample recordings demonstrate suppression of α7currents as early as 30 s after NRG 1β pulse (red trace). The maximum inhibition effect was reached at ~3 min (blue trace). Con, Control. ***D***, PTP inhibitor orthovanadate (1 mM) eliminated the recovery (sag back) of ACh currents during NRG 1β application. The maximum inhibition of α7 current by NRG 1β or NRG 1β plus orthovanadate in each case was taken as 100% and used to normalize the inhibition effects at other time points. Each point and bar represent mean and SEM, respectively, of results obtained from six neurons.

In interneurons that exhibited a biphasic response, inhibition of the fast response by NRG 1β was nearly complete (>95%) (Fig. 3*A–C*). The inhibition of the fast α7 nAChR response by NRG 1β was selective in that no change was observed in the size of the slow, non-α7 nAChR current (Fig. 3*A*, *C*) (supplemental Fig. S2, available at www.jneurosci.org as supplemental material).

ACh pulses were repeated at 3 min intervals to minimize receptor desensitization. Under these conditions, there was essentially no rundown of evoked currents over the course of >1 h (Figs. 2*B*, 3*B*). Thus, the observed attenuation of nicotinic response and partial recovery are not attributable to rundown or desensitization under our experimental protocol and recording conditions.

Time course of NRG 1β effect

To examine the time course of NRG 1β action more precisely, we studied the NRG 1β effect in dissociated hippocampal neurons maintained in monolayer cell culture. Rapid application of ACh evoked fast inward currents or biphasic responses (Fig. 3*C*) in 43 of the 69 (62%) large neurons observed. The ACh-evoked fast currents were bigger (800 ± 101 pA; $n = 43$) and faster than that induced in interneurons within hippocampal slices. This difference is likely attributable to the larger tip size of the ACh ejection pipette. NRG 1β was ejected (100 ms, 10 psi) from a second barrel of the same electrode that contains ACh. An effect of NRG 1β was observed as early as 30 s after the onset of the pulse. Three minutes after NRG 1β ejection, the fast α7 component was almost completely inhibited. As in slices, the NRG 1β action was selective in that non-α7 responses were not affected. Recovery after a brief pulse of NRG 1β was ~80% by 12 min (Fig. 3*C*).

PD 158780 blocked the suppression effect of NRG 1β on α7 nAChRs

Perfusion of hippocampal slice with NRG 1β together with a specific ErbB inhibitor PD 158780 (Fry et al., 1997; Rewcastle et al., 1998) at 10 μM abolished the NRG 1β inhibition of fast inward currents in interneurons that showed only fast (α7) nicotinic responses (Fig. 4*B*) and also in interneurons that showed mixed fast (α7) and slower (non-α7) responses (Fig. 4*D*). This result indicates that the same ErbB receptors that mediate long-term NRG actions are likely to mediate the rapid inhibition of α7 currents.

In the absence of NRG 1β, PD 158780 slightly increased the ACh-evoked α7 nAChR responses (Fig. 4*A*,*B*). The effect was small (10–15%), but it was consistent and sustained. This suggests a low level (endogenous) of ErbB kinase activity in the absence of exogenously applied NRG. In neurons that exhibited a biphasic response, PD 158780 also produced a small increase in the fast component (Fig. 4*C*,*D*).

Orthovanadate eliminated the recovery of the ACh currents in the presence of NRG 1β

The amplitude of the fast responses began to recover even in the continued presence of NRG 1β (Figs. 2*B*, 3*B*). Considering the

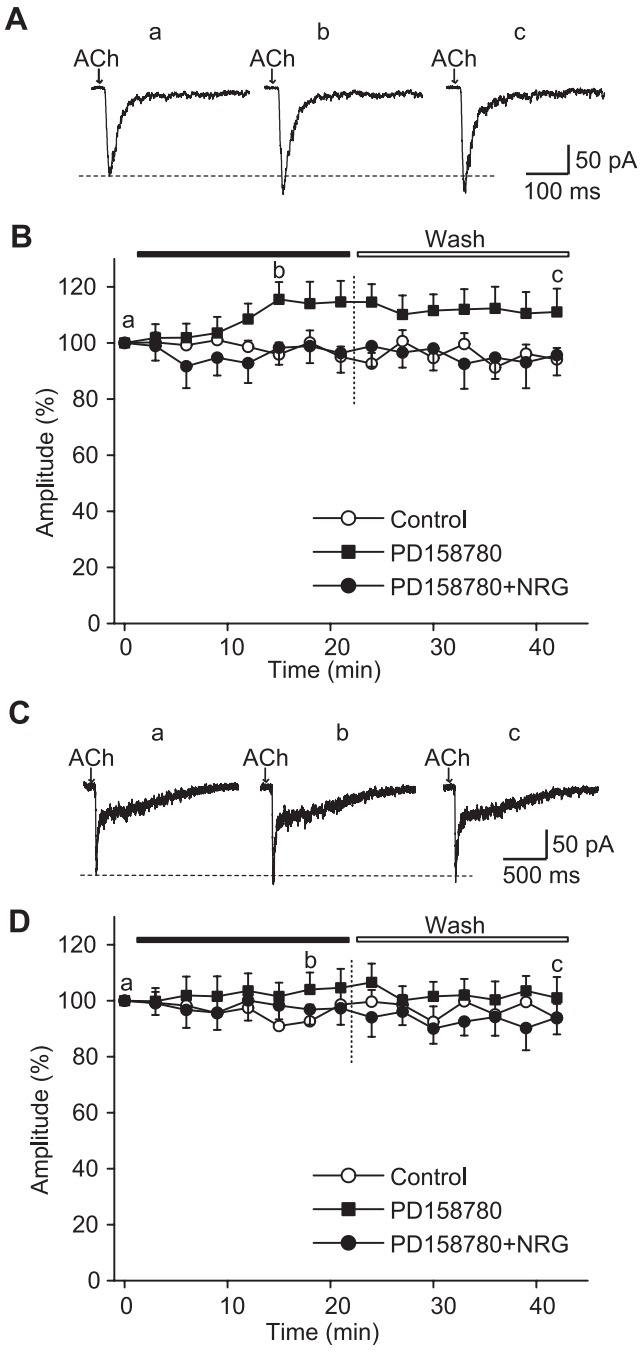

Figure 4. NRG 1β-induced suppression of α7 currents was blocked by ErbB inhibitor PD 158780 (10 μM). ***A***, Sample recordings of ACh-evoked fast currents before (***a***), 15 min after perfusion with PD 158780 (***b***), and 21 min after washout (***c***). ***B***, Averaged fast current amplitudes (percentage of $T = 0$; mean $\pm$ SEM; $n = 6$ cells) plotted versus time (minutes) in controls, in the presence of PD 158780, and in the presence of PD 158780 plus NRG 1β (5 nM). Note that PD 158780 alone produced a small but consistent increase in the α7 currents. ***C***, Sample recordings of ACh-evoked biphasic currents before (***a***), 18 min after perfusion with PD 158780 (***b***), and 21 min after washout (***c***). ***D***, Averaged fast α7 component amplitudes (percentage of $T = 0$; mean $\pm$ SEM; $n = 6$ cells) plotted versus time (minutes) in controls, in the presence of PD 158780, and in the presence of PD 158780 plus NRG 1β (5 nM). PD 158780 also blocked the effects of NRG 1β. A small increase in ACh currents in the presence of PD 158780 is evident.

likely role of tyrosine phosphorylation in NRG action, we hypothesized that the recovery of the ACh currents in the presence of NRG 1β was attributable to dephosphorylation of tyrosine residues. Indeed, application of orthovanadate, a protein phosphotyrosine phosphatase (PTP) inhibitor, at 1 mM along with NRG 1β reduced the "sag back" of α7 currents (supplemental Fig. S3*A*, available at www.jneurosci.org as supplemental material). The same result was obtained in neurons with complex responses (supplemental Fig. S3*B*, available at www.jneurosci.org as supplemental material). The prevention of recovery (sag back) of the ACh currents is more evident in the superimposed graph shown in Figure 3*D*.

Orthovanadate (1 mM) in the absence of NRG 1β slightly decreased the monophasic fast α7 currents (supplemental Fig. S3*A*, available at www.jneurosci.org as supplemental material), consistent with the notion that ongoing tyrosine phosphorylation modulates α7-mediated currents. The effect of orthovanadate was reversible after ~20 min washouts.

The actin cytoskeleton was involved in the NRG 1β suppression

Cytoskeleton proteins, such as actin, are important in the stability of surface neuronal α7 nAChRs (Shoop et al., 2000). To test whether the suppression by NRG 1β on α7 currents was affected by the integrity of actin cytoskeleton, we examined the effects of cytochalasin D (cyt D) (5 μM), an actin-depolymerizing agent and phalloidin (2 μM), an F-actin stabilizer on neurons grown in monolayer cell culture. After 15 min perfusion with cyt D, the fast α7-mediated response was slightly decreased, whereas the slow response was not affected. In the presence of cyt D, subsequent application of NRG 1β had no effect on ACh currents (Fig. 5*A*). Intracellular dialysis of the neurons with phalloidin from the patch pipette also prevented the suppression effect of NRG 1β on ACh currents (Fig. 5*B*).

NRG 1β increased α7 nAChRs internalization

In addition to application of agents that affect the actin cytoskeleton, we also assayed α7 nAChR internalization by confocal microscopy after labeling surface receptors with Alexa488-αBgt. Staining hippocampal neurons in culture with Alexa488-αBgt yielded specific labeling that was blocked by unlabeled αBgt (data not shown). Only surface α7 nAChRs were labeled with the Alexa488-αBgt because the toxin binding was performed on living cells before fixation and permeabilization. Serial optical sections along the *z*-axis confirmed that the staining was confined to the cell perimeter. Two broad categories of labeled neurons were observed in both control and NRG 1β-treated cultures. In control cultures, 70% ($n = 53$) of labeled neurons exhibited many intense clusters that could be readily observed on soma and proximal dendrites, and 30% exhibited fewer, less intense clusters (Fig. 6). In cultures treated with 5 nM NRG 1β for 9 min, only 44% ($n = 40$) of the labeled neurons were in the "intense clusters" category. Moreover, the number of clusters was reduced after NRG 1β treatment compared with controls in this category (Fig. 7*B*). In each experiment, the cells were fixed after Alexa488-αBgt labeling and then permeabilized to label all receptors (internal plus surface) with an anti-α7 nAChR antibody. The antibody sites detected with rhodamine-conjugated secondary antibody coincided with the surface Alexa488-αBgt sites detected through the cell interior (Fig. 7*A*). The specificity of the primary anti-α7 nAChR antibody was assayed by a blocking peptide (data not shown). The ratio of green-to-red fluorescence intensity was taken as a measure of surface-to-total α7 receptor density. This measure was also dramatically reduced by NRG 1β (Fig. 7*C*). As expected, over this short time course, we did not observe a significant change in total receptor levels. All of the changes described above were blocked by the specific ErbB inhibitor PD 158780 (10

μM) (Fig. 7*A–C*, NRG+PD), suggesting the mediation through ErbB receptor tyrosine kinases.

NRG 1β suppressed synaptic α7 nAChRs

It is important to determine whether the NRG 1β effects on exogenously ACh-induced currents were also evident in endogenous presynaptic released ACh-induced currents. Synaptic responses were elicited in CA1 SR interneurons by electrical stimulation of the afferent fibers in either SR or SO (Fig. 8*A*). To isolate synaptic potentials mediated by nAChRs, we blocked muscarinic, glutamatergic, and GABAergic synaptic responses with an inhibitor mixture containing atropine (1 μM), CNQX (20 μM), APV (50 μM), and picrotoxin (100 μM). Previous studies demonstrated that 5-HT_3 receptor and ATP receptor antagonists rarely affected the synaptic responses that were observed under these conditions (Alkondon et al., 1998). When holding at −65 mV, synaptically evoked responses in the presence of the inhibitor mixture could be detected in 4 of 32 cells. These fast inward residual currents were blocked by MLA (100 nM) (Fig. 8*B*), suggesting that they were nicotinic in nature and mediated by activation of α7 nAChRs. A similar low rate of success in detecting nicotinic synaptic transmission in hippocampal slices was observed in early studies (Alkondon et al., 1998; Frazier et al., 1998b). This probably reflects the difficulty in stimulating septohippocampal afferent fibers, the major cholinergic afferent system innervating hippocampal neurons.

In three experiments, bath application of NRG 1β (5 nM) reduced the amplitudes of MLA-sensitive EPSCs (Fig. 8*C*). Inhibition was evident at 3–6 min after the onset of bath perfusion and reached maximal of ~30% at ~10 min. The amplitude of the nicotinic EPSCs recovered to ~90% after 20 min wash.

Spontaneous synaptic currents were observed in the presence of the inhibitor mixture in 4 of 11 interneurons (data not shown). However, their amplitudes were too small (5–15 pA) and their frequencies, even in the presence of hypertonic sucrose (100 mM), were too low (0.5 Hz) to determine the effect of NRG 1β.

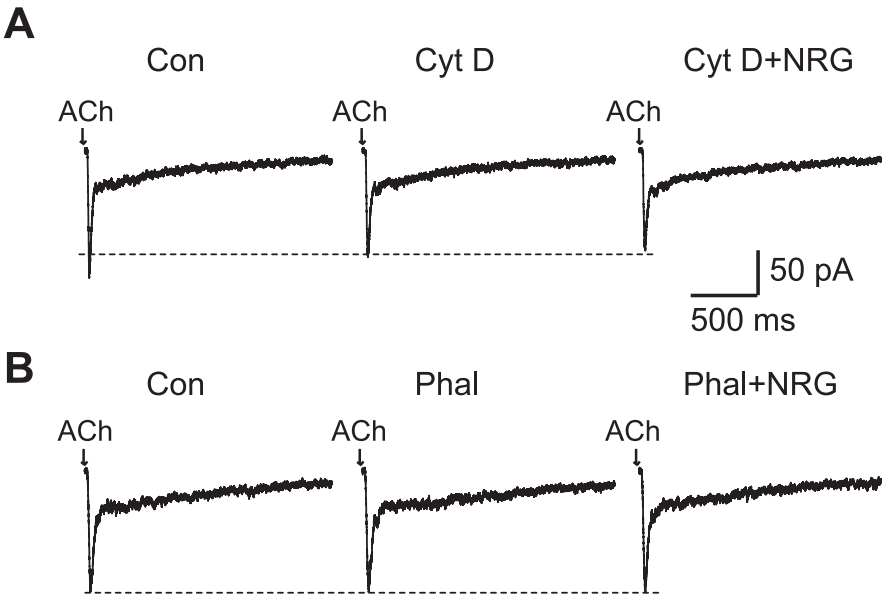

Figure 5. NRG 1β suppression of ACh currents was dependent on an intact actin cytoskeleton. ***A***, Representative current traces of ACh currents in control (Cont), 15 min after perfusion with cyt D (5 μM), and another 9 min after coapplication of cyt D and NRG 1β (5 nM). ***B***, Examples traces of ACh-induced currents without phalloidin (control), with phalloidin (2 μM; Phal) added to the intracellular solution, and subsequent perfusion with NRG 1β. The NRG 1β effect on ACh currents was prevented by the actin stabilizer phalloidin.

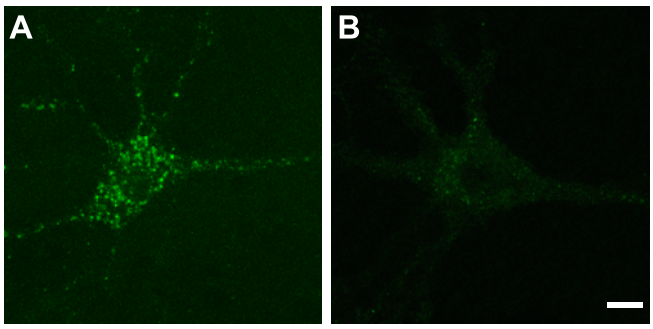

Figure 6. Two Alexa488-αBgt-labeled neurons in hippocampal cultures. ***A***, ***B***, These representative micrographs illustrate neurons expressing intense surface α7 nAChR clusters (***A***) and neurons showing fewer, less intense α7 nAChR clusters (***B***). Scale bar, 10 μm.

Discussion

The major finding of this study is that NRG 1β can produce a rapid decrease in α7 receptor-mediated ACh currents in hippocampal interneurons. The effect was dose dependent and it was selective in that non-α7 nAChRs were not affected. The down-regulation of functional α7 nAChRs was evident within 30 s, and this must be considered an upper limit. It may occur even faster in the intact brain after release of NRG from endogenous stores.

Given the speed of the effect, it cannot be attributable to a decrease in protein synthesis. A more likely explanation involves a change in the balance of receptor endocytosis and exocytosis. nAChRs undergo rapid trafficking between the surface membrane and intracellular pools (Liu et al., 2005). Trafficking is supported by our results after treatment with phalloidin and cyt D. It is also supported by the rapid decrease in the surface Alexa488-αBgt binding sites detected by confocal microscopy. Although the ratio of surface-to-total α7 nAChR declined, additional studies are needed to determine whether internalized receptors add to the intracellular store and are recycled or whether they are degraded.

Most relevant to our experiments are recent observations of rapid exocytosis of α7 nAChRs in rat hippocampal interneurons exposed to genistein, a nonspecific protein tyrosine kinase inhibitor (Cho et al., 2005). Genistein enhanced α7 currents and pervanadate, a PTP inhibitor, suppressed them. When α7 nAChRs were expressed in oocytes, the time constant of genistein was ~1.4 min. The increase in surface α7 receptors was associated with a corresponding decrease in intracellular receptors. Cho et al. (2005) found that this exchange between intracellular and surface pools was inhibited by botulinum toxin-A, implying a role for soluble *N*-ethylmaleimide-sensitive factor attachment protein receptor (SNARE), but the trafficking was apparently not dependent on an intact actin network.

Rapid trafficking of α7 nAChRs also occurs in spines that extend from chick ciliary ganglion neuron somata (Liu et al., 2005). The actin cytoskeleton and spine integrity as well as SNARE are required for nAChRs trafficking in the chick neurons

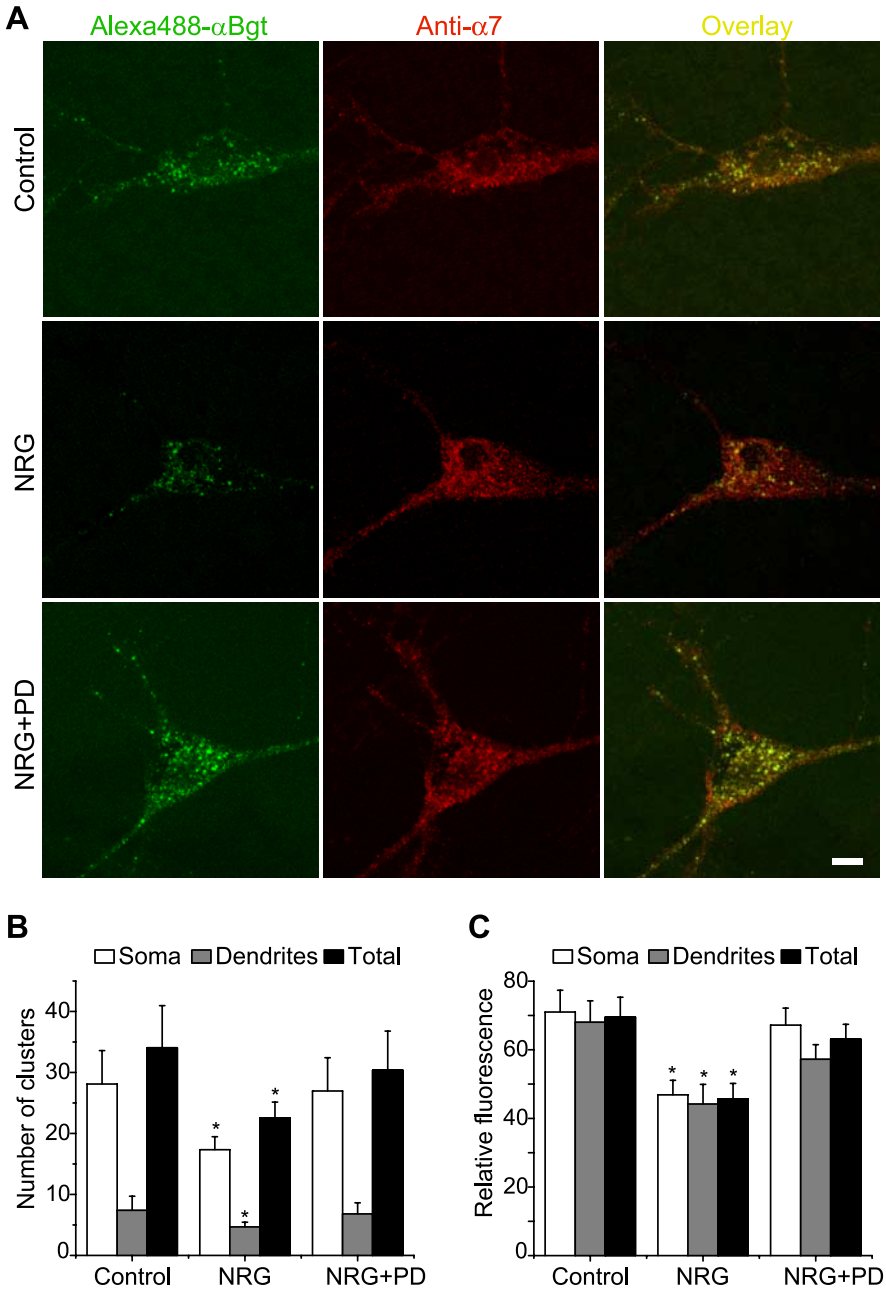

Figure 7. NRG 1β increased α7 nAChR internalization in cultured hippocampal neurons. ***A***, Representative micrographs showing the staining of surface and total α7 nAChRs in control neurons (top row) and in neurons after treatment with NRG 1β (middle row) or NRG 1β plus PD 158780 (bottom row; PD). Cell stained first (green) with Alexa488-αBgt (left column) and then fixed, permeabilized, and costained (red) with an anti-α7 nAChR antibody (middle column) and shown in overlay (right column), revealing surface clusters of receptor that colabeled with both markers (yellow). Antibody staining also showed intracellular receptor protein not seen with the Alexa488-αBgt staining performed on the intact cell. Scale bar, 10 μm. ***B***, NRG 1β regulation of surface α7 nAChR clusters. The numbers of α7 nAChR clusters on soma (within two 15 $\times$ 15 μm areas), two to four dendrites (within 50 μm starting from the soma), and total (soma plus dendrites) were measured on each neuron. ***C***, Quantitative analysis of relative (surface/total ratio) α7 nAChR fluorescence intensity in neurons treated without or with NRG in the absence or presence of PD 158780. Data for ***B*** and ***C*** represent the mean $\pm$ SEM (*$p < 0.05$, Student's t test). $n = 40$–53 cells for each treatment.

(Shoop et al., 2000; Liu et al., 2005). The specificity for α7 subunits observed in our studies of NRG β1 was evident in untreated chick neurons (Liu et al., 2005) and in oocytes expressing nicotinic receptor subunits (Cho et al., 2005).

It is possible that a change in single-channel conductance or channel open time or probability of opening also contribute to the rapid NRG-induced decrease in α7 currents. Tyrosine phosphorylation increases the rate of receptor desensitization of nAChRs isolated from *Torpedo californica* membranes and reconstituted in liposomes (Hopfield et al., 1988). It is not yet clear whether the same phenomenon occurs in neuronal nicotinic receptors, nor is it clear whether the effect of NRG 1β on neuronal receptors is attributable to phosphorylation of the receptor itself or to other proteins that modulate nAChR function. There are three tyrosine residues in the intracellular loop of α7 subunits, but they are not essential for the action of genistein or pervanadate (Cho et al., 2005).

ErbB kinases are the only known NRG receptors, which leads us to suggest that these enzymes are involved in the rapid NRG action. The efficacy of PD 158780 in blocking downregulation of α7 receptors induced by NRG is consistent with this assumption. Downstream molecules in this rapid signaling pathway remain to be investigated.

We cannot explain the different efficacies of NRG in blocking fast currents in mid-SR interneurons (~45%) compared with SR/SLM border interneurons (~90%). It might be attributable to different density/distribution of ErbB receptors or to different types of ErbB receptor or to differences in downstream signaling pathways that perhaps lead to endocytosis. In any case, this interesting difference should be pursued at the synaptic level.

Changes in glutamate receptor trafficking and associated change in synaptic efficacy are now well documented (Malinow and Malenka, 2002; Bredt and Nicoll, 2003; Wenthold et al., 2003). Indeed, NRG 1β promotes internalization of AMPA receptors in CA1 pyramidal cells, resulting in depotentiation after induction of long-term potentiation (Kwon et al., 2005). In the prefrontal cortex, NRG 1β reduces NMDA currents by enhancing NR1 internalization (Gu et al., 2005). Other rapid NRG 1 actions include increase of calcium-activated potassium channels (Chae et al., 2005) and modulating *in vivo* entorhinal-hippocampal synaptic transmission (Roysommuti et al., 2003).

Long-term (≥48 h) treatment of hippocampal neurons with NRG 1β produces a robust increase in the number of surface nAChRs and an increase in α7 receptor-mediated currents in hippocampal interneurons (Liu et al., 2001; Kawai et al., 2002). It will be important to determine whether this long-term effect is attributable to a change in gene expression or whether it reflects a delayed posttranslational process.

Long-term exposure to NRG regulates the expression of other types of ligand-gated channels. NRG 1β induces expression of the $GABA_A$ receptor β2 subunit mRNA (Rieff et al., 1999; Xie et al., 2004) and NMDA receptor 2C subunit mRNA (Ozaki et al.,

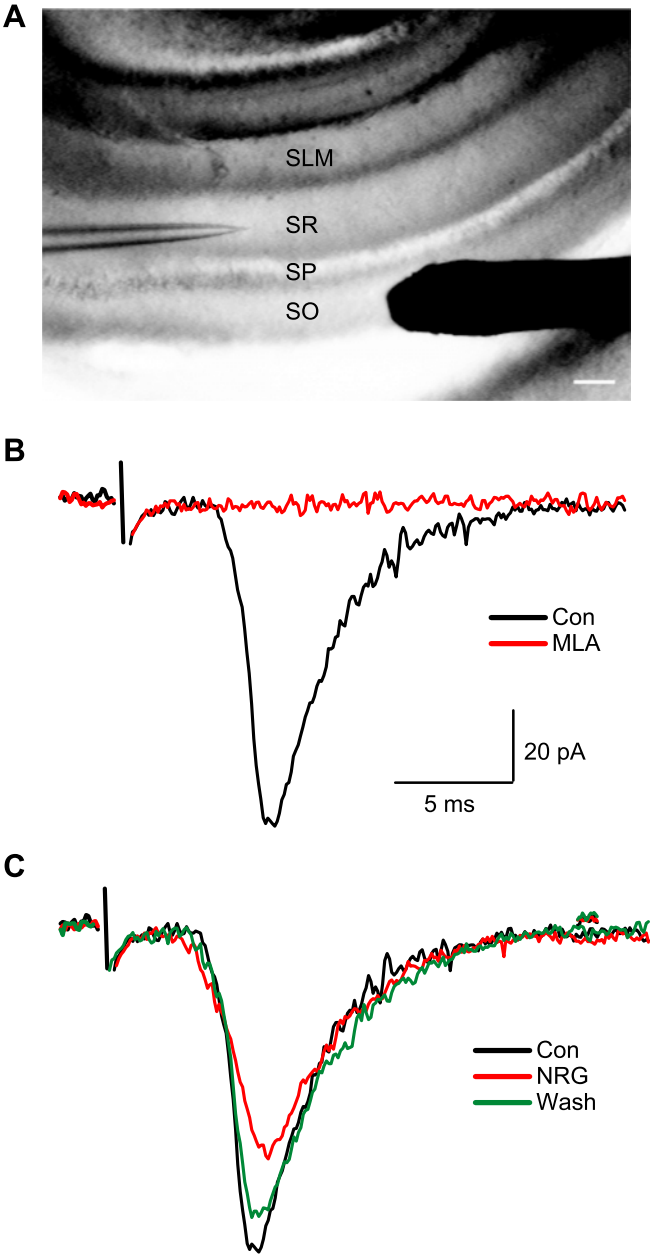

Figure 8. NRG 1β reduced α7 nicotinic EPSCs in hippocampal slices. ***A***, A low-power view of the hippocampal slice preparation showing the location of the stimulation electrode (right), which, in this experiment, is located on the surface of the SO ~300 μm from the recording electrode (left). Scale bar, 100 μm. ***B***, A fast EPSC recorded in the presence of atropine (1 μM), CNQX (20 μM), APV (50 μM), and picrotoxin (100 μM; black trace). This current was blocked by MLA (100 nM; red trace). ***C***, Sample recordings of nicotinic synaptic currents before (black trace), 9 min after NRG 1β (5 nM) perfusion (red trace), and 21 min after washout (green trace). Con, Control.

1997) in cerebellar granule cells. NRG 1 reduces the expression of $GABA_A$ receptor α subunit mRNA in hippocampal slices (Okada and Corfas, 2004). Therefore, NRG can have effects on neuronal ion channel gene expression.

We also found evidence for activation of ErbB kinases in the hippocampus in the absence of added NRG. There may be a low level of endogenous NRG in tissue slices prepared from the hippocampus. Cholinergic axons, a likely source of NRG, might issue from local interneurons or from neurons in the medial septal nucleus that project to the hippocampus. NRG mRNA has been detected in the hippocampus and in the medial septal nucleus (Chen et al., 1994; Corfas et al., 1995; Law et al., 2004; Okada and Corfas, 2004). Non-NRG ligands must also be considered. ErbB4 in tumor cells or heterologous system can be activated by other members of the EGF family (Beerli and Hynes, 1996; Bianco et al., 1999).

It is also possible ErbB kinases might dimerize and become activated in the absence of any ligand (Boerner et al., 2001). Although ErbB4 has been detected in hippocampal interneurons (Garcia et al., 2000; Huang et al., 2000; Gerecke et al., 2001; Okada and Corfas, 2004), we do not know the density or the distribution of these receptors so it is difficult to evaluate the possibility of spontaneous dimerization and activation. PD 158780 does not distinguish between activation of liganded and unliganded kinases because this agent is not a competitive inhibitor of NRG binding. Rather, it acts at the intracellular ATP binding site (Fry et al., 1997; Rewcastle et al., 1998).

It will be important to study the effects of acute and chronic exposure to NRG on local circuit function and plasticity. We observed significant suppression of presumed α7-mediated EPSCs. These were difficult experiments because of the low incidence of nicotinic EPSCs (Alkondon et al., 1998; Frazier et al., 1998b). Most stimuli in the presence of muscarinic, ionotropic glutamate, and GABA receptors antagonists elicited no EPSCs at all. This may reflect the fact that incoming axons are severed in slices or that the axons are highly dispersed. Given the density of cholinergic terminals in the hippocampus, we predict that effects of synaptically released ACh are ubiquitous and profound.

There is little doubt that α7 nAChR activation can affect interneuronal synaptic transmission. This might be attributable to depolarization at or near the target neuron axon hillock or by enhanced calcium influx at or near target nerve terminals. We predict that the acute inhibition of α7 currents in hippocampal interneurons would lead to decreased release of GABA at some GABAergic synapses and induce a change in the balance between excitatory and inhibitory drives.

In moving beyond rapid action of NRG on single cells, one must deal with the complexity of neural circuits in the hippocampus (Ji and Dani, 2000). In addition, one must take the long-term effects as well as the acute actions of NRG into account.

References

Alkondon M, Pereira EF, Albuquerque EX (1998) alpha-bungarotoxin- and methyllycaconitine-sensitive nicotinic receptors mediate fast synaptic transmission in interneurons of rat hippocampal slices. Brain Res 810:257–263.

Beerli RR, Hynes NE (1996) Epidermal growth factor-related peptides activate distinct subsets of ErbB receptors and differ in their biological activities. J Biol Chem 271:6071–6076.

Bianco C, Kannan S, De Santis M, Seno M, Tang CK, Martinez-Lacaci I, Kim N, Wallace-Jones B, Lippman ME, Ebert AD, Wechselberger C, Salomon DS (1999) Cripto-1 indirectly stimulates the tyrosine phosphorylation of erb B-4 through a novel receptor. J Biol Chem 274:8624–8629.

Boerner JL, Danielsen A, McManus MJ, Maihle NJ (2001) Activation of Rho is required for ligand-independent oncogenic signaling by a mutant epidermal growth factor receptor. J Biol Chem 276:3691–3695.

Bredt DS, Nicoll RA (2003) AMPA receptor trafficking at excitatory synapses. Neuron 40:361–379.

Buonanno A, Fischbach GD (2001) Neuregulin and ErbB receptor signaling pathways in the nervous system. Curr Opin Neurobiol 11:287–296.

Chae KS, Oh KS, Dryer SE (2005) Growth factors mobilize multiple pools of KCa channels in developing parasympathetic neurons: role of ADP-ribosylation factors and related proteins. J Neurophysiol 94:1597–1605.

Chen MS, Bermingham-McDonogh O, Danehy Jr FT, Nolan C, Scherer SS, Lucas J, Gwynne D, Marchionni MA (1994) Expression of multiple neuregulin transcripts in postnatal rat brains. J Comp Neurol 349:389–400.

Cho CH, Song W, Leitzell K, Teo E, Meleth AD, Quick MW, Lester RA (2005) Rapid upregulation of α7 nicotinic acetylcholine receptors by tyrosine dephosphorylation. J Neurosci 25:3712–3723.

Corfas G, Rosen KM, Aratake H, Krauss R, Fischbach GD (1995) Differential expression of ARIA isoforms in the rat brain. Neuron 14:103–115.

Dodt HU, Zieglgansberger W (1990) Visualizing unstained neurons in living brain slices by infrared DIC-videomicroscopy. Brain Res 537:333–336.

Falls DL (2003) Neuregulins: functions, forms, and signaling strategies. Exp Cell Res 284:14–30.

Falls DL, Rosen KM, Corfas G, Lane WS, Fischbach GD (1993) ARIA, a protein that stimulates acetylcholine receptor synthesis, is a member of the neu ligand family. Cell 72:801–815.

Fischbach GD, Rosen KM (1997) ARIA: a neuromuscular junction neuregulin. Annu Rev Neurosci 20:429–458.

Frazier CJ, Rollins YD, Breese CR, Leonard S, Freedman R, Dunwiddie TV (1998a) Acetylcholine activates an α-bungarotoxin-sensitive nicotinic current in rat hippocampal interneurons, but not pyramidal cells. J Neurosci 18:1187–1195.

Frazier CJ, Buhler AV, Weiner JL, Dunwiddie TV (1998b) Synaptic potentials mediated via α-bungarotoxin-sensitive nicotinic acetylcholine receptors in rat hippocampal interneurons. J Neurosci 18:8228–8235.

Freund TF, Buzsaki G (1996) Interneurons of the hippocampus. Hippocampus 6:347–470.

Fry DW, Nelson JM, Slintak V, Keller PR, Rewcastle GW, Denny WA, Zhou H, Bridges AJ (1997) Biochemical and antiproliferative properties of 4-[ar(alk)ylamino]pyridopyrimidines, a new chemical class of potent and specific epidermal growth factor receptor tyrosine kinase inhibitor. Biochem Pharmacol 54:877–887.

Garcia RA, Vasudevan K, Buonanno A (2000) The neuregulin receptor ErbB-4 interacts with PDZ-containing proteins at neuronal synapses. Proc Natl Acad Sci USA 97:3596–3601.

Gerecke KM, Wyss JM, Karavanova I, Buonanno A, Carroll SL (2001) ErbB transmembrane tyrosine kinase receptors are differentially expressed throughout the adult rat central nervous system. J Comp Neurol 433:86–100.

Gu Z, Jiang Q, Fu AK, Ip NY, Yan Z (2005) Regulation of NMDA receptors by neuregulin signaling in prefrontal cortex. J Neurosci 25:4974–4984.

Hopfield JF, Tank DW, Greengard P, Huganir RL (1988) Functional modulation of the nicotinic acetylcholine receptor by tyrosine phosphorylation. Nature 336:677–680.

Huang YZ, Won S, Ali DW, Wang Q, Tanowitz M, Du QS, Pelkey KA, Yang DJ, Xiong WC, Salter MW, Mei L (2000) Regulation of neuregulin signaling by PSD-95 interacting with ErbB4 at CNS synapses. Neuron 26:443–455.

Ji D, Dani JA (2000) Inhibition and disinhibition of pyramidal neurons by activation of nicotinic receptors on hippocampal interneurons. J Neurophysiol 83:2682–2690.

Jones S, Yakel JL (1997) Functional nicotinic ACh receptors on interneurones in the rat hippocampus. J Physiol (Lond) 504:603–610.

Kawai H, Zago W, Berg DK (2002) Nicotinic α7 receptor clusters on hippocampal GABAergic neurons: regulation by synaptic activity and neurotrophins. J Neurosci 22:7903–7912.

Kwon OB, Longart M, Vullhorst D, Hoffman DA, Buonanno A (2005) Neuregulin-1 reverses long-term potentiation at CA1 hippocampal synapses. J Neurosci 25:9378–9383.

Law AJ, Shannon Weickert C, Hyde TM, Kleinman JE, Harrison PJ (2004) Neuregulin-1 (NRG-1) mRNA and protein in the adult human brain. Neuroscience 127:125–136.

Lemke G (1996) Neuregulins in development. Mol Cell Neurosci 7:247–262.

Liu Y, Ford B, Mann MA, Fischbach GD (2001) Neuregulins increase α7 nicotinic acetylcholine receptors and enhance excitatory synaptic transmission in GABAergic interneurons of the hippocampus. J Neurosci 21:5660–5669.

Liu Z, Tearle AW, Nai Q, Berg DK (2005) Rapid activity-driven SNARE-dependent trafficking of nicotinic receptors on somatic spines. J Neurosci 25:1159–1168.

MacVicar BA (1984) Infrared video microscopy to visualize neurons in the in vitro brain slice preparation. J Neurosci Methods 12:133–139.

Malinow R, Malenka RC (2002) AMPA receptor trafficking and synaptic plasticity. Annu Rev Neurosci 25:103–126.

McQuiston AR, Madison DV (1999) Nicotinic receptor activation excites distinct subtypes of interneurons in the rat hippocampus. J Neurosci 19:2887–2896.

Okada M, Corfas G (2004) Neuregulin1 downregulates postsynaptic GABAA receptors at the hippocampal inhibitory synapse. Hippocampus 14:337–344.

Ozaki M, Sasner M, Yano R, Lu HS, Buonanno A (1997) Neuregulin-beta induces expression of an NMDA-receptor subunit. Nature 390:691–694.

Pawelzik H, Hughes DI, Thomson AM (2002) Physiological and morphological diversity of immunocytochemically defined parvalbumin- and cholecystokinin-positive interneurones in CA1 of the adult rat hippocampus. J Comp Neurol 443:346–367.

Rewcastle GW, Murray DK, Elliott WL, Fry DW, Howard CT, Nelson JM, Roberts BJ, Vincent PW, Showalter HD, Winters RT, Denny WA (1998) Tyrosine kinase inhibitors. 14. Structure-activity relationships for methylamino-substituted derivatives of 4-[(3-bromophenyl)amino]-6-(methylamino)-pyrido[3,4-d]pyrimidine (PD 158780), a potent and specific inhibitor of the tyrosine kinase activity of receptors for the EGF family of growth factors. J Med Chem 41:742–751.

Rieff HI, Raetzman LT, Sapp DW, Yeh HH, Siegel RE, Corfas G (1999) Neuregulin induces $GABA_A$ receptor subunit expression and neurite outgrowth in cerebellar granule cells. J Neurosci 19:10757–10766.

Roysommuti S, Carroll SL, Wyss JM (2003) Neuregulin-1beta modulates in vivo entorhinal-hippocampal synaptic transmission in adult rats. Neuroscience 121:779–785.

Shoop RD, Yamada N, Berg DK (2000) Cytoskeletal links of neuronal acetylcholine receptors containing α7 subunits. J Neurosci 20:4021–4029.

Sudweeks SN, Yakel JL (2000) Functional and molecular characterization of neuronal nicotinic ACh receptors in rat CA1 hippocampal neurons. J Physiol (Lond) 527:515–528.

Talmage DA, Role LW (2004) Multiple personalities of neuregulin gene family members. J Comp Neurol 472:134–139.

Usdin TB, Fischbach GD (1986) Purification and characterization of a polypeptide from chick brain that promotes the accumulation of acetylcholine receptors in chick myotubes. J Cell Biol 103:493–507.

Wenthold RJ, Prybylowski K, Standley S, Sans N, Petralia RS (2003) Trafficking of NMDA receptors. Annu Rev Pharmacol Toxicol 43:335–358.

Wietasch K (1997) Regulation of neuronal nicotinic acetylcholine receptors in the interpeduncular nucleus. PhD thesis, Harvard University.

Xie F, Raetzman LT, Siegel RE (2004) Neuregulin induces GABAA receptor beta2 subunit expression in cultured rat cerebellar granule neurons by activating multiple signaling pathways. J Neurochem 90:1521–1529.

Yang X, Kuo Y, Devay P, Yu C, Role L (1998) A cysteine-rich isoform of neuregulin controls the level of expression of neuronal nicotinic receptor channels during synaptogenesis. Neuron 20:255–270.